

## **MS JCI 42666 RG version 4**

### **Supplemental Data**

#### **Integration of a Notch-dependent mesenchymal gene program and Bmp2-driven cell invasiveness regulates murine cardiac valve formation**

Luis Luna-Zurita, Belén Prados, Joaquim Grego-Bessa, Guillermo Luxán, Gonzalo del Monte, Alberto Benguría, Ralf H. Adams, José María Pérez-Pomares and José Luis de la Pompa

### **Supplemental Methods**

#### **Generation of mouse *Cdh5(PAC)-Cre<sup>ERT2</sup>* strain**

The inducible line *Cdh5(PAC)-Cre<sup>ERT2</sup>* was generated as follows. The RPCI21 PAC library (Geneservice, UK), containing 129/SvevTACfBr mouse spleen genomic DNA in a pPAC4 vector (1), was screened by filter hybridization with a radioactive mouse *Cadh5* (*VE-Cadherin*) cDNA probe. A cDNA encoding Tamoxifen-inducible Cre recombinase (2) upstream of a polyadenylation signal sequence and an FRT-flanked Ampicilin resistance cassette was introduced by recombineering (3) into the start codon of *Cadh5* in PAC clone 353-G15. After Flp-mediated excision of the Ampicilin resistance cassette in bacteria, the resulting constructs were validated by PCR analysis and used in circular form for pronuclear injection into fertilized mouse oocytes. Founders, identified by PCR genotyping, were screened by timed matings with *ROSA26R* reporter animals (4). For a more detailed description about the generation and characterization of this driver line please see (5).

**Strain genotyping.** For primers and conditions see Table S2.

#### **4-hydroxy-tamoxifen (4-OHT) induction**

Cre activity was induced by two consecutive intraperitoneal injections of pregnant females at days 9.5 and 10.5 post coitum with 100  $\mu$ l tamoxifen solution

(Sigma, T5648; 10 mg ml<sup>-1</sup>; generated by diluting a 10×tamoxifen stock in 100% ethanol with peanut oil).

### **Scanning Electron Microscopy**

Mouse embryos were fixed in 1% paraformaldehyde (PFA), 1% glutaraldehyde in PBS and postfixed in 1% OsO<sub>4</sub>. Embryos were then dehydrated, paraffin-embedded and sectioned with a Leica microtome. Tissues were dewaxed in xylene, washed in 100% ethanol and dried. All samples were gold sputtered and scanned a JEOL JSM-840 scanning electron microscope (operated between 10 and 20 kV). Images were captured with ScanVision 1.0 software (Röntec) directly coupled to the microscope.

### **Histology, lacZ staining and In situ Hybridization**

Hematoxylin/eosin (H&E) and LacZ stainings were performed according to standard protocols. Whole-mount in situ hybridization (WISH) were as described (6). Details for probes will be provided on request.

### **Cell Culture**

Bovine Aortic Endothelial Cells (BAEC) were cultured in 0.1% gelatin-coated plates in complete DMEM-Glutamax medium (Invitrogen) containing 10% FBS and antibiotics (37 °C, 5% CO<sub>2</sub>). BAECs and HEK293T were starved for 24 h in medium containing 0.5% FBS prior to treatment for 4 h with 20 ng/ml BMP2 (R&D Systems). Cells were subsequently treated for 3 h with 20 μM of proteasome inhibitor MG132 (Calbiochem), harvested and processed for Western blot. BMP2-treated BAECs analyzed for immunodetection of Snail1 and phospho-Gsk3β were not treated with MG132. For RNA expression analysis, BAEC were cultured in 0.5% FBS for 24h, followed by 2h-incubation with BMP2 and NF-κB inhibitor (Calbiochem, 18 μM) followed by treatment with BMP2.

### **Immunostainings**

Tissue sections were stained for CD31/PECAM with a commercial antibody (1:100 dilution; 557355, BD Pharmingen) according to standard protocols (7). Staining with rat anti-MLC2v antibody (1:50(8), anti-Snail1 hybridoma supernatant (1:100; (9), or rabbit anti-NIICD antibody (1:100; Cell Signaling, see(10) was amplified with a

tyramide signal amplification kit (TSA™; Perkin Elmer). The anti-N1ICD antibody recognizes Val1744, which is exposed upon  $\gamma$ -secretase cleavage of Notch1. This epitope is not present in the construct used to generate the *R26N1ICD* transgenic mice (11), and thus this antibody cannot be used to detect ectopic N1ICD expression in these mice. BAEC were fixed with 4% paraformaldehyde in PBS for 10 minutes at RT. Cells were incubated with the anti-snail1 supernatant (1:200) and anti-phospho-GSK3 $\beta$  (1:100, Cell Signaling) followed by incubation with anti-mouse or anti-rabbit biotinylated IgG antibodies (1:100) (Vector Labs) and tyramide signal amplification. Stained sections or cells were analyzed with an Olympus BX51 microscope fitted with a Nikon DP71 camera and Cella controller software, or with an Olympus Fluoview FV-1000 confocal microscope. Quantification of intensity in Snail1 and p-Gsk3 $\beta$  immunofluorescence was done using the software Adobe PhotoShop 10.0, measuring the average signal per nucleus (in the case of Snail1) or per cell (in the case of p-Gsk3 $\beta$ ). The results of the Snail1 and p-Gsk3 $\beta$  immunofluorescence quantification are shown as the relation between control and BMP2-treated cells.

### **Confocal imaging**

Confocal images of stained explants and tissue sections were acquired with an Olympus Fluoview FV-1000 laser-scanning confocal microscope. Images of GFP proteins and FITC stainings were obtained with a 488 nm krypton-argon laser; Cyan3 with a 543 nm helium-neon laser; and DAPI with a 405 nm diode laser. Images of stained explants were collected as z-stacks with 1.50  $\mu$ m spacing between each plane. Images were fused and assembled to produce movies, lateral sections and Z-projections using ImageJ 1.32J software. Image treatments were with Adobe Photoshop 10.0.

### **RNA isolation and semiquantitative RT-PCR**

E9.5 or E11.5 wt and mutant embryos were dissected in ice-cold PBS and the whole heart or left ventricles were separated from the rest of the body and total RNA was purified using Trizol (Invitrogen). ENC from explants were isolated using collagenase type II (Sigma), and RNA was purified with Trizol. BAEC cells (subconfluent p30 plate) were isolated and total RNA was purified using Trizol. cDNA was synthesized with SuperScript III First Strand (Invitrogen), with 1 $\mu$ g total RNA per reaction. For primers and conditions see Table S3.

## Microarray Hybridization and Scanning

Biotinylated cRNA was synthesized from total RNA obtained from triplicate WT and *Tie2-Cre;R26NIICD* E9.5 heart samples using the 3' Amplification One-cycle Target labeling kit (Affymetrix, Santa Clara, CA). Briefly, first strand cDNA was produced by reverse transcribing 2 µg of RNA from a 24mer oligodT primer with a T7 RNA polymerase promoter site added to the 3' end. After second strand synthesis, biotin-labeled cRNA was produced by *in vitro* transcription using T7 RNA polymerase and biotinylated nucleotides. The cRNAs were hybridized in triplicate to Affymetrix Mouse Genome 430 2.0 microarrays (Affymetrix, Santa Clara, CA). Arrays were washed and stained according to the manufacturer's standard protocols, and were scanned in an Affymetrix GeneChip® Scanner 3000. Data were analyzed with affylmaGUI R software (12). The robust Multi-array Analysis (RMA) algorithm was used for background correction, normalization and expression level summarization (13). Differential expression analysis was performed using *limma* (14) included in the affylmGUI package. P-values were corrected for multiple testing using the Benjamini-Hochberg method (15) Functional, network and pathway analyses were conducted with Ingenuity Pathway Analysis software (Ingenuity Systems®, [www.ingenuity.com](http://www.ingenuity.com))

## Western Blot

Total protein extracts of cultured cells or E9.5 wt and transgenic atria-AVC or left ventricles were obtained in 25 mM Tris-HCl and 1% SDS lysis buffer containing protease inhibitors. Equal amounts of protein (20 µg) were separated by SDS-PAGE and transferred to PVDF membranes (Millipore) under standard conditions. Blots were incubated with anti-snail1 hybridoma supernatant (1:40 (9)), anti-GSK3β and anti-phospho-GSK3β (1:1000, Cell Signaling), anti-phospho-p44/42 Erk1/2 (Thr202/Tyr204) (1:5000, Cell Signaling) and anti-tubulin (1:10,000, Sigma). Bound HRP-conjugated secondary antibodies were detected by ECL (GE-Healthcare).

## References

1. Osoegawa, K., Tateno, M., Woon, P.Y., Frengen, E., Mammoser, A.G., Catanese, J.J., Hayashizaki, Y., and de Jong, P.J. 2000. Bacterial artificial chromosome libraries for mouse sequencing and functional analysis. *Genome Res* 10:116-128.

2. Feil, R., Wagner, J., Metzger, D., and Chambon, P. 1997. Regulation of Cre recombinase activity by mutated estrogen receptor ligand-binding domains. *Biochem Biophys Res Commun* 237:752-757.
3. Copeland, N.G., Jenkins, N.A., and Court, D.L. 2001. Recombineering: a powerful new tool for mouse functional genomics. *Nat Rev Genet* 2:769-779.
4. Soriano, P. 1999. Generalized lacZ expression with the ROSA26 Cre reporter strain. *Nat Genet* 21:70-71.
5. Wang, Y., Nakayama, M., Pitulescu, M.E., Schmidt, T.S., Bochenek, M.L., Sakakibara, A., Adams, S., Davy, A., Deutsch, U., Luthi, U., et al. 2010. Ephrin-B2 controls VEGF-induced angiogenesis and lymphangiogenesis. *Nature* 465:483-486.
6. Timmerman, L.A., Grego-Bessa, J., Raya, A., Bertran, E., Perez-Pomares, J.M., Diez, J., Aranda, S., Palomo, S., McCormick, F., Izpisua-Belmonte, J.C., et al. 2004. Notch promotes epithelial-mesenchymal transition during cardiac development and oncogenic transformation. *Genes Dev* 18:99-115.
7. Krebs, L.T., Xue, Y., Norton, C.R., Shutter, J.R., Maguire, M., Sundberg, J.P., Gallahan, D., Closson, V., Kitajewski, J., Callahan, R., et al. 2000. Notch signaling is essential for vascular morphogenesis in mice. *Genes Dev* 14:1343-1352.
8. Franco, D., Markman, M.M., Wagenaar, G.T., Ya, J., Lamers, W.H., and Moorman, A.F. 1999. Myosin light chain 2a and 2v identifies the embryonic outflow tract myocardium in the developing rodent heart. *Anat Rec* 254:135-146.
9. Franci, C., Takkunen, M., Dave, N., Alameda, F., Gomez, S., Rodriguez, R., Escriva, M., Montserrat-Sentis, B., Baro, T., Garrido, M., et al. 2006. Expression of Snail protein in tumor-stroma interface. *Oncogene* 25:5134-5144.
10. Del Monte, G., Grego-Bessa, J., Gonzalez-Rajal, A., Bolos, V., and De La Pompa, J.L. 2007. Monitoring Notch1 activity in development: Evidence for a feedback regulatory loop. *Dev Dyn* 236:2594-2614.
11. Murtaugh, L.C., Stanger, B.Z., Kwan, K.M., and Melton, D.A. 2003. Notch signaling controls multiple steps of pancreatic differentiation. *Proc Natl Acad Sci U S A* 100:14920-14925.
12. Wettenhall, J.M., Simpson, K.M., Satterley, K., and Smyth, G.K. 2006. affyLmGUI: a graphical user interface for linear modeling of single channel microarray data. *Bioinformatics* 22:897-899.
13. Irizarry, R.A., Hobbs, B., Collin, F., Beazer-Barclay, Y.D., Antonellis, K.J., Scherf, U., and Speed, T.P. 2003. Exploration, normalization, and summaries of high density oligonucleotide array probe level data. *Biostatistics* 4:249-264.
14. Smyth, G.K. 2004. Linear models and empirical bayes methods for assessing differential expression in microarray experiments. *Stat Appl Genet Mol Biol* 3:Article3.
15. Benjamini, Y.a.H., Y. 1995. Controlling the False Discovery Rate: A Practical and Powerful Approach to Multiple Testing. . *Journal of the Royal Statistical Society, Series B (Methodological)* 57:289-300.
16. Grego-Bessa, J., Luna-Zurita, L., del Monte, G., Bolos, V., Melgar, P., Arandilla, A., Garratt, A.N., Zang, H., Mukoyama, Y.S., Chen, H., et al. 2007. Notch signaling is essential for ventricular chamber development. *Dev Cell* 12:415-429.
17. Nakagawa, O., Nakagawa, M., Richardson, J.A., Olson, E.N., and Srivastava, D. 1999. HRT1, HRT2, and HRT3: a new subclass of bHLH transcription factors

- marking specific cardiac, somitic, and pharyngeal arch segments. *Dev Biol* 216:72-84.
18. Fischer, A., Steidl, C., Wagner, T.U., Lang, E., Jakob, P.M., Friedl, P., Knobloch, K.P., and Gessler, M. 2007. Combined loss of Hey1 and HeyL causes congenital heart defects because of impaired epithelial to mesenchymal transition. *Circ Res* 100:856-863.
  19. Lamar, E., Deblandre, G., Wettstein, D., Gawantka, V., Pollet, N., Niehrs, C., and Kintner, C. 2001. Nrarp is a novel intracellular component of the Notch signaling pathway. *Genes Dev* 15:1885-1899.
  20. Krebs, L.T., Deftos, M.L., Bevan, M.J., and Gridley, T. 2001. The Nrarp gene encodes an ankyrin-repeat protein that is transcriptionally regulated by the notch signaling pathway. *Dev Biol* 238:110-119.
  21. Moens, C.B., Stanton, B.R., Parada, L.F., and Rossant, J. 1993. Defects in heart and lung development in compound heterozygotes for two different targeted mutations at the N-myc locus. *Development* 119:485-499.

## Supplemental Figure Legends

**Supplemental Figure 1. Ectopic Notch pathway activation in endocardium affects cardiac development and leads to Notch target gene up-regulation.** (A) Transverse section of the heart of an E9.5 *Tie2-Cre;R26R* embryo showing intense  $\beta$ -gal staining in endocardium. (B) General view of an E9.5 WT heart. (C) General view of a *Tie2-Cre;NIICD* transgenic heart. (D, E) Detail of AVC. Note mesenchymal cells in WT (D, arrow) and transgenic AVC (E, arrow). (F) Detail of WT left ventricle. Arrow points to trabeculae. (G) Detail of *Tie2-Cre;NIICD* left ventricle. Note poorly developed trabeculae (arrow). (H) RT-PCR of E9.5 WT and *Tie2-Cre;NIICD* hearts. (I-T) WISH analysis of Notch1 target genes expression in the avc and lv regions at E9.5. (I, J) *Hey1* is expressed in atrial endocardium and myocardium of WT heart, while *Tie2-Cre;NIICD* embryos show *Hey1* expression expanded to the entire endocardium. (K, L) *Hey2* expression in endocardium and the myocardium of the ventricular compact zone is the same in WT and *Tie2-Cre;NIICD* embryos, though expression was slightly increased in *Tie2-Cre;NIICD* hearts (H). (M, N) *Hey1* is transcribed in some cells of avc endocardium in WT hearts; in *Tie2-Cre;NIICD* embryos *Hey1* transcription extends throughout the endocardium. (O, Q, S) *Dll4*, *Nrarp* and *c-Myc* are transcribed in WT heart at the base of ventricular endocardium and at low levels in avc. (P, R, T) *Tie2-Cre;NIICD* heart shows *Dll4*, *Nrarp* and *c-Myc* transcription throughout the endocardium. Arrows mark endocardium. ra, right atrium; avc, atrioventricular canal; lv, left ventricle; Scale bar, 10  $\mu$ m.

**Supplemental Figure 2. Chamber and EMT markers expression in *Tie2-Cre;NIICD* embryos.** (A-J) WISH analysis of E9.5 hearts (detail). (A, B) *Anf* transcription is restricted to cameral myocardium in WT and transgenic hearts (arrows) and it is excluded from the endocardium (arrowheads). The bracket marks the AVC. (C, D) *Irx5* expression in trabecular endocardium (arrowheads). Expression is much weaker in *Tie2-Cre;NIICD* hearts. (E, F) *Bmp2* is expressed in AVC myocardium (arrows) in WT (E) and *Tie2-Cre;NIICD* embryos (F). (G, H) *Twist1* is restricted to mesenchymal AVC cells (arrowheads) in both WT (G) and transgenic embryos (H). (I, J) *Has2* is expressed in the mesenchymal AVC cells in WT (I) and transgenic hearts (J, arrowheads). (K) RT-PCR. The expression of endothelial (*CD31*), myocardial (*Mlc2v* and *Mlc2a*) and cameral markers (*Anf* and *Chisel*) is unaffected. The endocardial trabecular markers *Irx5* is down-regulated. Note the slight reduction in *Bmp2*

transcription in transgenic embryos at E9.5 while at E10.5, expression is recovered. Expression of the EMT markers *Twist1* and *Has2* is unaffected in transgenic hearts. at, atrium; avc, atrioventricular canal; lv, left ventricle. Scale bar, 10  $\mu$ m.

**Supplemental Figure 3. The vasculature of *Tie2-Cre;NIICD* embryos ectopically expresses arterial markers.** (A-F) WISH analysis of E9.5 embryos. (A, B) *Dll4* is expressed in the WT dorsal aorta endothelium (arrow) but not in the anterior cardinal vein (A). In *Tie2-Cre;NIICD* embryos (B), *Dll4* is expressed in both dorsal aorta and anterior cardinal vein endothelium (arrows). (C, D) WT expression of the arterial marker *Efnb2* is expanded from the dorsal aorta endothelium (C, arrows) to the anterior cardinal vein endothelium in *Tie2-Cre;NIICD* embryos heart (D, arrows). (E, F) Expression in the anterior cardinal vein of the venous marker *Ephb4* in WT embryos (E, arrow) is reduced in *Tie2-Cre;NIICD* embryos (F, arrow). da, dorsal aorta; acv, anterior cardinal vein. Scale bar, 20  $\mu$ m.

**Supplemental Figure 4. EMT and mesenchyme markers expression is up-regulated in *Tie2-Cre;NIICD* embryos .** (A-H) WISH in E9.5 WT and *Tie2-Cre;NIICD* embryos. Details of the heart. (A, B) Expression of *Sox9* is expanded from the AVC endocardium and mesenchyme (A, arrow) to the ventricular endocardium in the transgenic heart (arrowhead in B). (C, D) Normal expression of *Periostin* is expanded from the AVC mesenchyme (C, D, arrows) to the ventricular endocardium in the transgenic heart (D, arrowhead). A similar pattern is seen for *Bmp6* (E, F) and *Cxcr4* (G, H). (I) RT-PCR in E9.5 WT and *Tie2-Cre;NIICD* hearts. All markers are up-regulated. avc, atrioventricular canal; lv, left ventricle. Scale bar, 20 $\mu$ m.

**Supplemental Figure 5. E9.5 *Tie2-Cre;NIICD* embryos ectopically express mesenchyme markers in chamber endocardium.** (A-H) General views of panels shown in Figure 1I-P. Arrowheads, AVC myocardium; arrows, AVC endocardium; thick arrow, ventricular endocardium. (A, B) Normal *Tgfb2* expression in AVC and ectopic expression in ventricular endocardium of *Tie2-Cre;NIICD* embryos. (C, D) WT embryos express *Snail1* in AVC endocardium and mesenchyme (C), *Tie2-Cre;NIICD* embryos show ectopic expression in ventricular endocardium (D). *Tie2-Cre;NIICD* hearts also show ectopic ventricular expression of *Snail2* (F) and *Twist2* (H). avc, atrioventricular canal; lv, left ventricle. Scale bar, 20  $\mu$ m.

**Supplemental Figure 6. *Tie2-Cre;NIICD* AVC explants show increased migratory ability.** General views of (A) WT and (B) *Tie2-Cre;NIICD* AVC explants. The dotted lines indicate the plane of section corresponding to the lateral images shown below. All explants were fixed and stained with phalloidin-FITC (green) and anti- $\alpha$ -SMA-Cy3 (red) to detect both the actin cytoskeleton and mesenchymal cells, and counterstained with DAPI (blue). Arrowheads mark transformed endocardial cells. In *Tie2-Cre;NIICD* AVC, transformed cells scatter over the gel surface (C) Quantitative analysis of transformation index. The invasive capacity (3D TI) of the transgenic explants is unaffected but the 2D TI (surface scattered cells as a proportion of all cells of endocardial origin) is increased ( $P=4.4 \times 10^{-2}$ ). (D) RT-PCR of endocardial cells from AVC WT and transgenic explants. Note that the up-regulation of genes involved in EMT (*Tgfb2*, *Snail1*, *Snail2*, *Vimentin*) and Notch targets (*Hey1*, *Hey2*, *Heyl*). Scale bar, 200  $\mu$ m.

**Supplemental Figure 7. *Cdh5(PAC)-Cre<sup>ERT2</sup>;NIICD* embryos and derived ventricular explants undergo partial EMT.** (A, B) Whole mount views of E11.5 WT and transgenic embryos, tamoxifen-induced from E9.5-E10.5. Note haemorrhage in the heart (arrowhead) and surrounding region of the *Cdh5(PAC)-Cre<sup>ERT2</sup>;NIICD* embryo. The dotted lines indicate the plane of sections shown in (D-I). (C) RT-PCR of WT and transgenic hearts. (D-I) H+E stained heart sections. (D) View of WT left ventricle and AVC. (E) Detail of WT AVC; note the numerous mesenchymal cells (arrowheads) in cushion regions. (F) Detail of ventricle; note the flattened endocardial cells (arrows) lining the trabecular myocardium. (G) View of *Cdh5(PAC)-Cre<sup>ERT2</sup>;NIICD* left ventricle and AVC. (H) Detail of AVC; cushions are less densely populated by mesenchymal cells (arrowheads). Note also a somewhat more rounded morphology. (I) Detail of left ventricle; note the fibroblastic, star-like morphology of trabecular endocardial cells (arrows). (J, K) General views of E11.5 ventricular explants after three days of culture. The dotted lines indicate the plane of section corresponding to the lateral views shown below. All explants were triple-stained as in Figure S6. (J) WT explant. The endocardium grows as a monolayer. (K) *Cdh5(PAC)-Cre<sup>ERT2</sup>;NIICD* explant. Note the scattered endocardial cells on the collagen surface that do not invade the matrix. (L) Quantification of 2D and 3D TI. Note the significantly increased migratory capacity of transgenic cells (2D index;  $P=2.7 \times 10^{-4}$ ). e, endocardium; m,

myocardium. Scale bar, 250 $\mu$ m (A, B), 20 $\mu$ m (D, G), 20 $\mu$ m (E, H), 10 $\mu$ m (F, I), 200 $\mu$ m (J, K).

**Supplemental Figure 8. *Nkx2.5-Cre;NIICD* and *cTnT-Cre;NIICD* embryos show cardiac dysmorphology and absence of AVC mesenchyme.** (A) Transverse section of an E9.5 *Nkx2.5-Cre;R26R* heart stained with X-gal. LacZ expression is detected in the myocardium, endocardium and in the mesenchymal cells of the heart (arrowhead). (B) Lateral view of an E9.5 *Nkx2.5-Cre;NIICD* heart showing EGFP expression throughout the heart. (C,D) Comparison of WT (C) and representative *Nkx2.5-Cre;NIICD* (D) E9.5 whole mount embryos. The dotted line in D indicates the plane of histological section. (E) H+E stained transverse heart section of an E9.5 *Nkx2.5-Cre;NIICD* embryo. (F) Detail of AVC; note the lack of mesenchymal cells in the cushion (asterisk). (G) Detail of the left ventricle; note the poorly developed trabeculae (arrows) and the space separating trabecular endocardium and myocardium. For a comparison with a WT heart see Figure S1. (H) Transverse section of an E9.5 *cTnT-Cre;R26R* heart stained with X-gal. LacZ expression is detected throughout the myocardium. (I) Lateral view of an E9.5 *cTnT-Cre;NIICD* heart showing myocardial EGFP expression. (J,K) Comparison of WT (J) and representative *cTnT-Cre;NIICD* (K) E10.5 whole mount embryos. The dotted line in K indicates the plane of histological section. (L) H+E stained transverse heart section of an *cTnT-Cre;NIICD* embryo at E.10.5. (M) Detail of the AVC; note the lack of mesenchymal cells in the cushion space (asterisk). (N) Detail of the left ventricle; trabeculae (arrow) appear to be unaffected. Scale bar, 20  $\mu$ m (A, E, H, L); 50  $\mu$ m (B, I); 100  $\mu$ m (C, D, J, K); 20  $\mu$ m (F, G, M,N).

**Supplemental Figure 9. Notch-dependent and Hey-mediated *Bmp2* inhibition in endocardium and AVC myocardium.** (A, H) WISH analysis of E9.5. (A, B) *Hey1* cardiac expression. In WT embryos (A), *Hey1* is expressed in the endocardium (arrow) and the myocardium (arrowhead) of the atrium. In *RBPJk* embryos (B), *Hey1* is detected in the atrial myocardium (arrowhead) but not in the atrial endocardium (arrow). (C, D) *Hey2* cardiac expression. In WT embryos (C), *Hey2* is expressed in the compact zone of the ventricular myocardium (arrowhead) and throughout the endocardium (arrow). In *RBPJk* embryos (D), *Hey2* is detected in the ventricular myocardium (arrowhead) but not in the endocardium (arrow). (E, F) *Hey1* is expressed in the WT AVC endocardium (E) but not in the *RBPJk* endocardium (F). (G, H) *Bmp2* cardiac expression. In WT embryos (G), *Bmp2* is expressed in the AVC myocardium

(arrowhead). In *RBPJk* embryos (H), myocardial *Bmp2* transcription (arrowhead) is unaffected. In contrast, these mutants show ectopic *Bmp2* expression throughout the endocardium (arrow) and myocardial expression is normal (arrowhead). (I) RT-PCR analysis. *RBPJk* mutants show reduced *Hey2* expression and increased *Bmp2* expression. at, atrium; lv, left ventricle; the bracket marks the atrio-ventricular canal (avc). Scale bar, 20  $\mu\text{m}$ .

**Supplemental Figure 10. NF- $\kappa$ B inhibition reduces the BMP2-dependent WT ventricular transformation.** All explants were triple-stained as in Figure S6. Lateral sections of explants are shown below. Arrowheads mark invading ENC. (A) BMP2-treated WT ventricular explants. (B) Inhibition of NF- $\kappa$ B activity in BMP2-treated WT ventricular explants. (C) Quantitative analysis of transformation index. The 2D ( $P=3.54 \times 10^{-5}$ ) and 3D ( $P=0.03$ ) TI is reduced with the NF- $\kappa$ B inhibitor treatment. (D) RT-PCR analysis of endocardial cells from BMP2 and BMP2 + NF- $\kappa$ B inhibitor-treated WT ventricular explants. NF- $\kappa$ B inhibition reduces *Snail1* expression. Scale bar, 200  $\mu\text{m}$ .

**Supplemental Figure 11. Myocardial *Bmp2* deletion disrupts AVC development and leads to reduced *Notch1* and *Snail1* transcription.** (A) E10.5 WT embryo. The dotted line indicates the plane of section shown in (C). (B) E10.5 *cTnT-Cre;Bmp2<sup>lox</sup>* embryo. The dotted line indicates the plane of section shown in (D). Note the reduced size and the accumulated blood in the heart and cephalic region. (C, D) H+E staining. General views. (E) Detail of WT AVC; note the numerous mesenchyme cells (arrowhead) in the cushion. (F) Detail of corresponding region in *cTnT-Cre;Bmp2<sup>lox</sup>* heart. The arrowheads mark flattened endocardial cells. There is no sign of cushion tissue or mesenchyme. avc, atrioventricular canal, avc. Scale bar, 100  $\mu\text{m}$  (A, B), 10  $\mu\text{m}$  (C, D, E, F).

**Supplemental Figure 12. Interactions between Notch, Hey proteins and Bmp2 during cardiac patterning.** (A) Left, E9.5 WT heart. Myocardium (dark grey) and endocardium (light grey) are shown, with N1ICD activity (red) labelling specific endocardial regions in chambers and AVC. Middle, myocardial expression domains of *Hey1*, *Hey2* and *Bmp2* pattern the chambers and AVC. Atrial *Hey1* (blue) and ventricular *Hey2* (green) expression confines *Bmp2* (orange) to prospective valve myocardium. Right, endocardial expression domains. N1ICD activates in a region-

specific manner *Hey1* (blue), *Hey2* (green) and *Heyl* (yellow) to pattern the AVC and chambers and repress *Bmp2*. (B) Left, E9.5 *Tie2-Cre;NIICD* heart. NIICD (red) is ectopically expressed throughout the endocardium. Middle, myocardial expression of *Hey* is unaffected and AVC and chambers patterning is normal. Right, Ectopic NIICD in endocardium activates *Hey1-l*, and AVC features are expanded to the ventricles. *Bmp2* is repressed. (C) Left, E9.5 *cTnT-Cre;NIICD* heart. NIICD is ectopically expressed throughout the myocardium, while endocardial expression is normal. Middle, *Hey1* is ectopically expressed in the myocardium and represses *Bmp2* in this tissue. AVC patterning is lost. Right, endocardial *NIICD* and *Hey1-l* are unaffected and patterning is normal. (D) Left, E9.5 *RBPJk* mutant heart. Middle, myocardial expression of *Hey1* and *Hey2* is unaffected and *Bmp2* is repressed in chamber myocardium. Patterning is normal. Right, endocardial expression of *Hey1-l* is down-regulated and *Bmp2* is ectopically expressed throughout the endocardium. Patterning is lost. at, atrium; avc, atrio-ventricular canal; lv, left ventricle.

## Supplemental Videos Legends

In all videos the explants are viewed from the top. Explants were stained with phalloidin-FITC (green) and anti- $\alpha$ -SMA-Cy3 (red) to detect both the actin cytoskeleton and mesenchymal cells and counterstained with DAPI (blue). The myocardium is a compact mass on top of ENC.

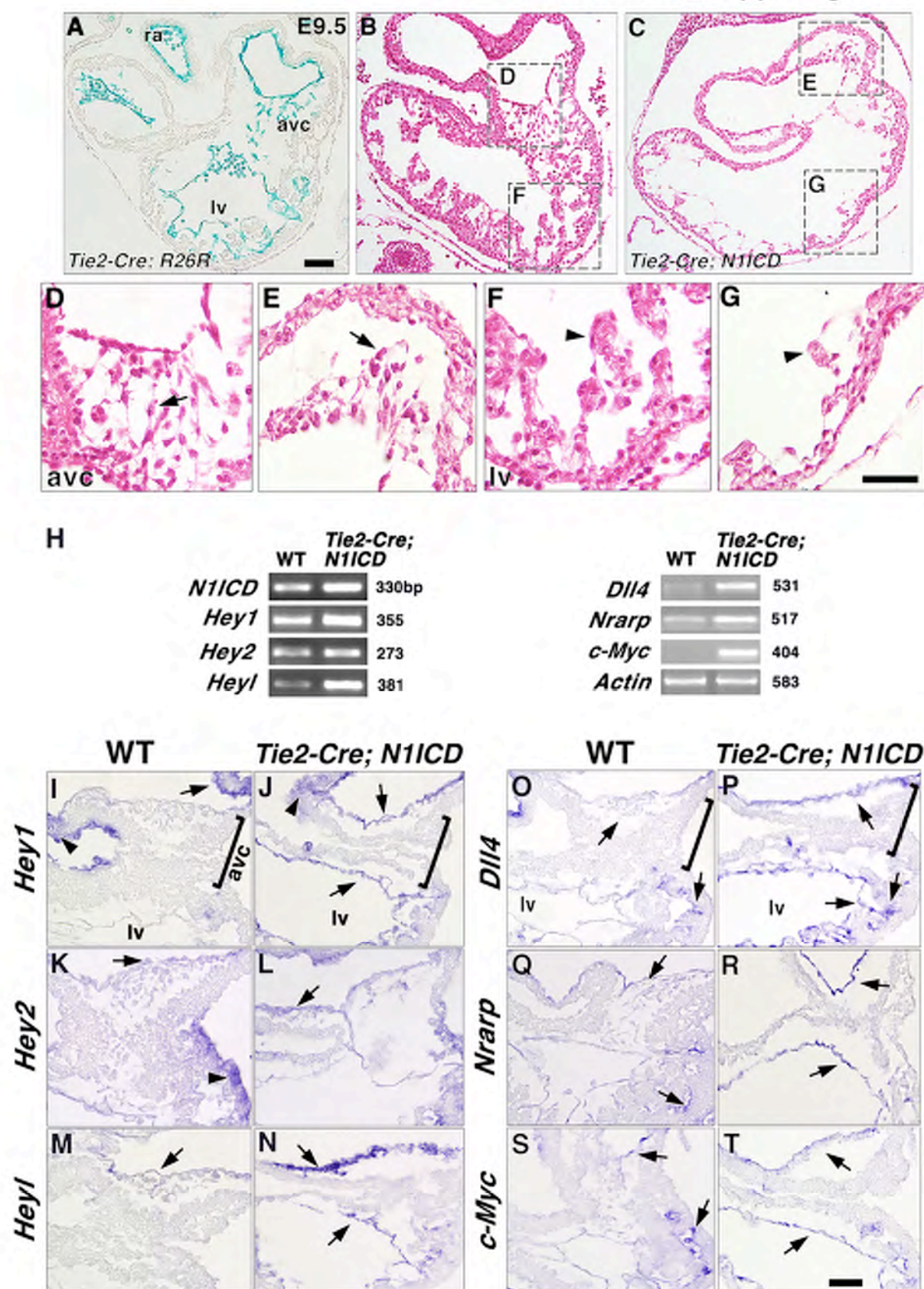
**Supplemental Video 1: WT and *Tie2-Cre;NIICD* AVC explants on collagen gel.** In both genotypes a large fraction of endocardial cells undergo EMT, extending cellular processes and migrating over and inside the gel. After confocal analysis and quantification, it was observed an increased migratory capacity of transgenic ENC.

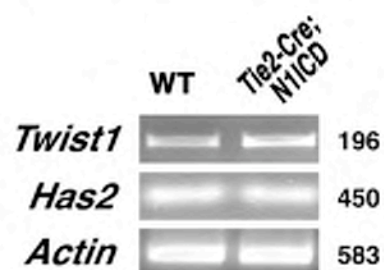
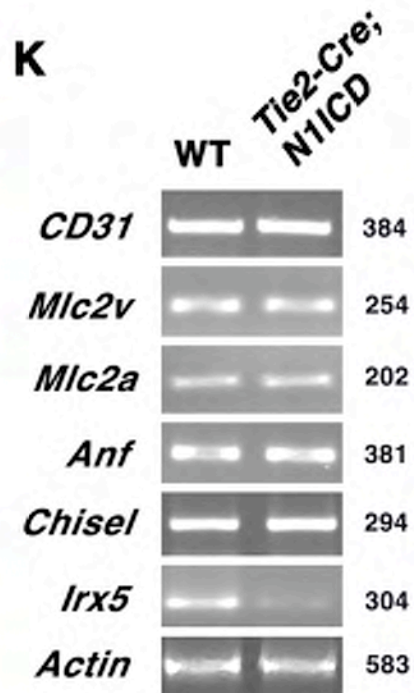
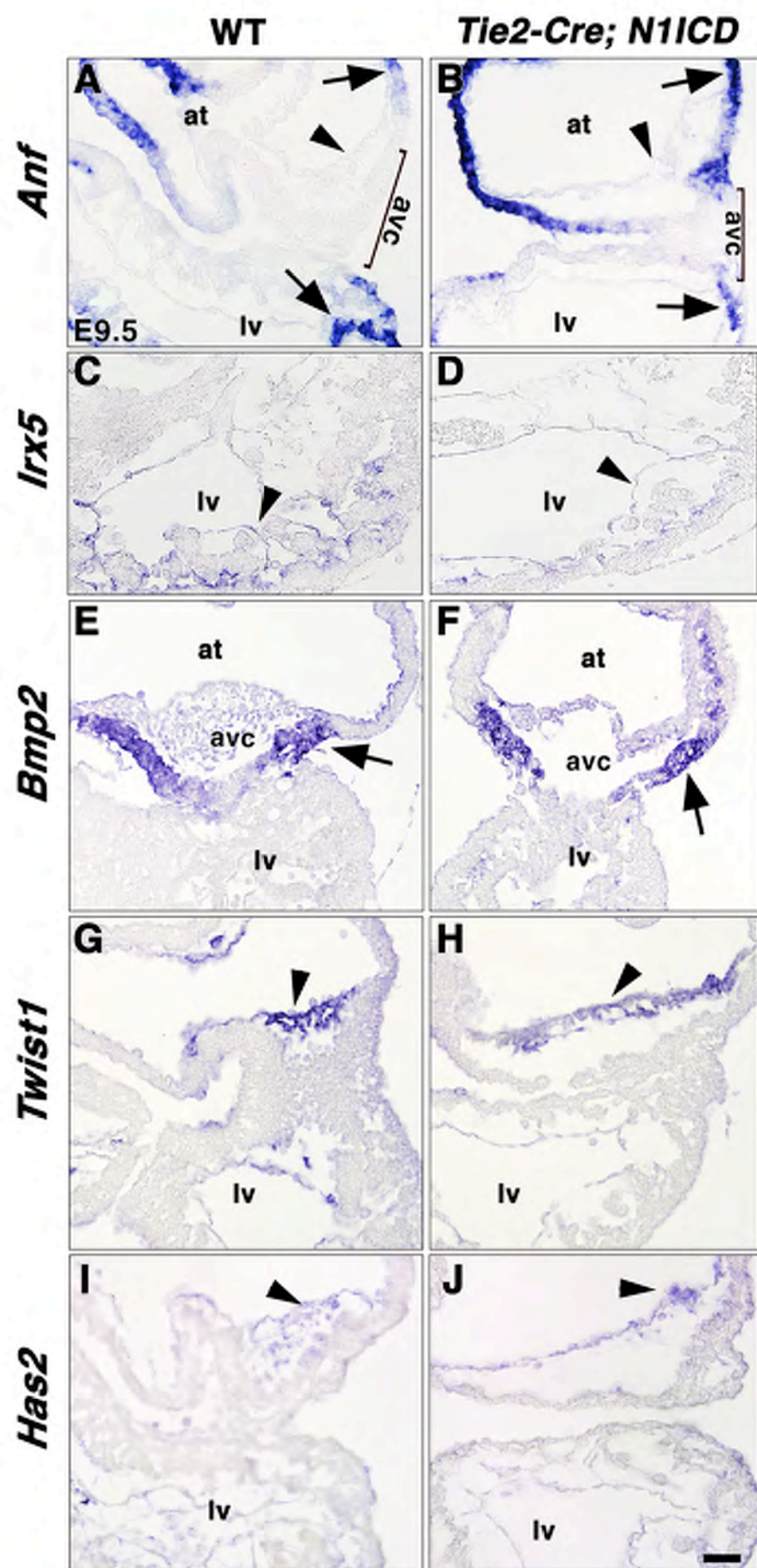
**Supplemental Video 2: WT and *Tie2-Cre;NIICD* ventricular explants.** In WT explants ENC grow as a coherent monolayer while in *Tie2-Cre;NIICD* explants ENC transform and migrate across the gel. Confocal analysis indicated that these ENC undergo partial EMT, as they do not invade the collagen gel.

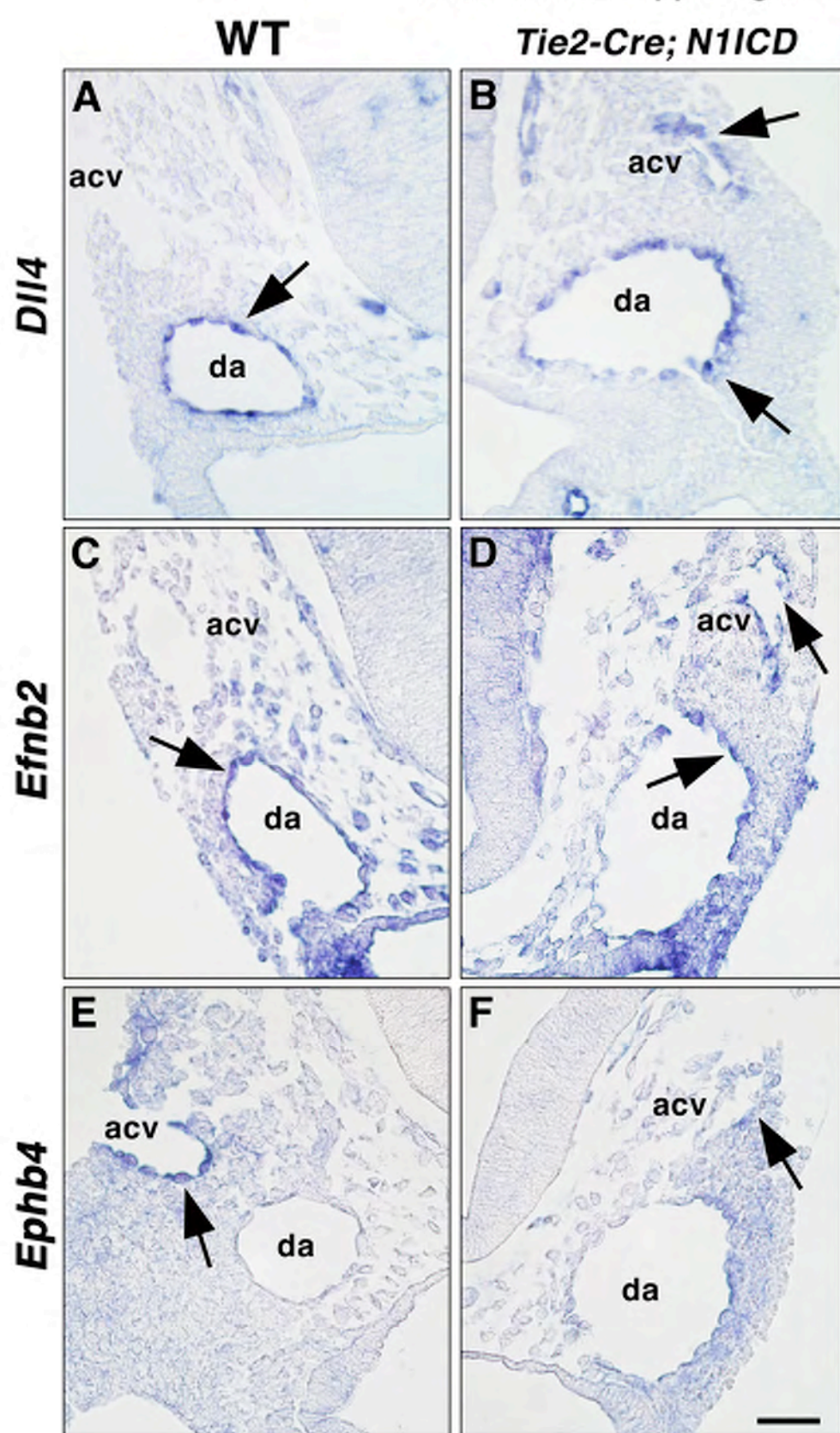
**Supplemental Video 3: WT and *Tie2-Cre;NIICD* ventricular explants cultured with BMP2.** In both genotypes addition of BMP2 to the medium induces complete EMT of ENC cells. Confocal analysis indicated that these transformed ENC invade the collagen.

**Supplemental Video 4: *Nkx2.5-Cre;NIICD* AVC explants cultured in the absence or presence of BMP2.** Confocal analysis indicated in the absence of BMP2, ENC undergo partial EMT with ENC migrating but not invading the collagen gel. Upon BMP2 addition to the medium, transform ENC become fully invasive.

Luna-Zurita\_Suppl. Figure 1

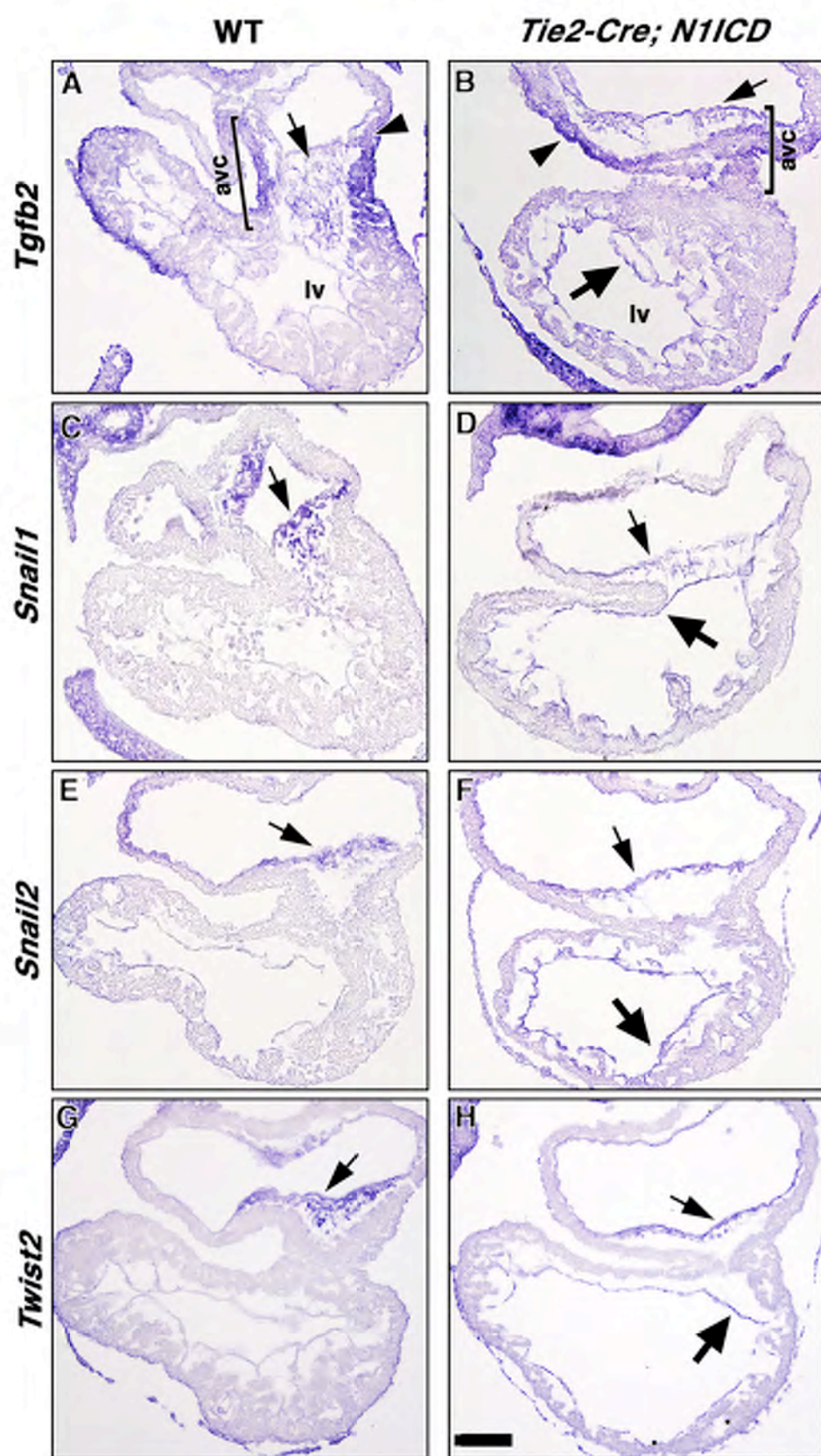


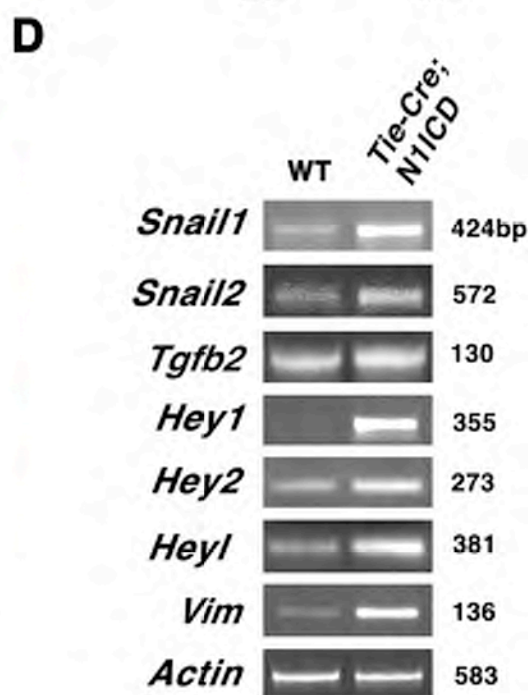
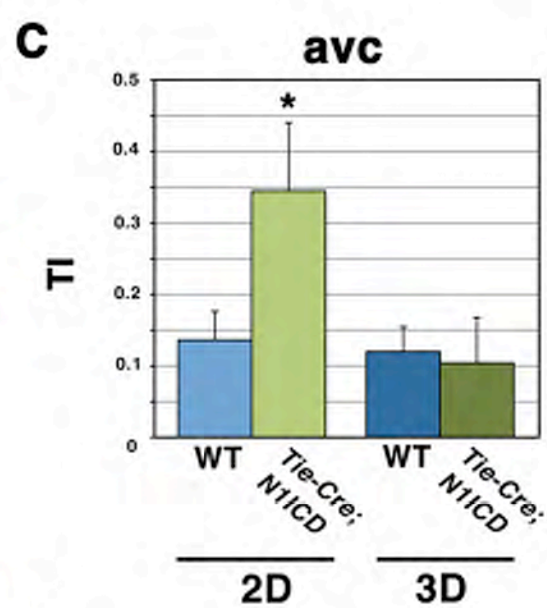
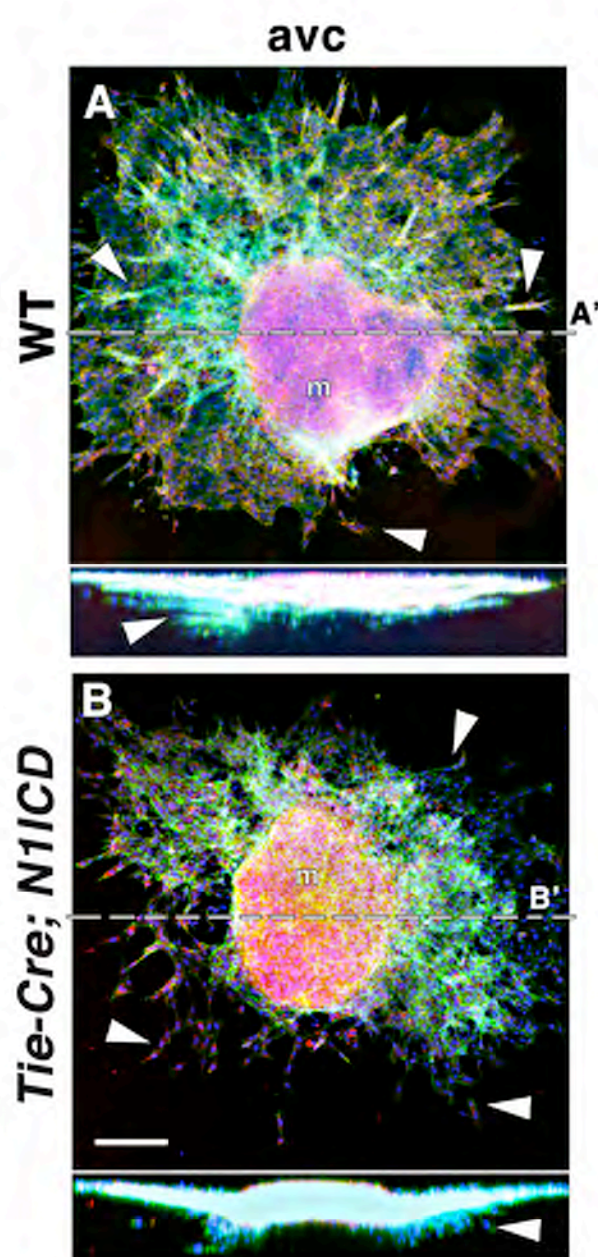




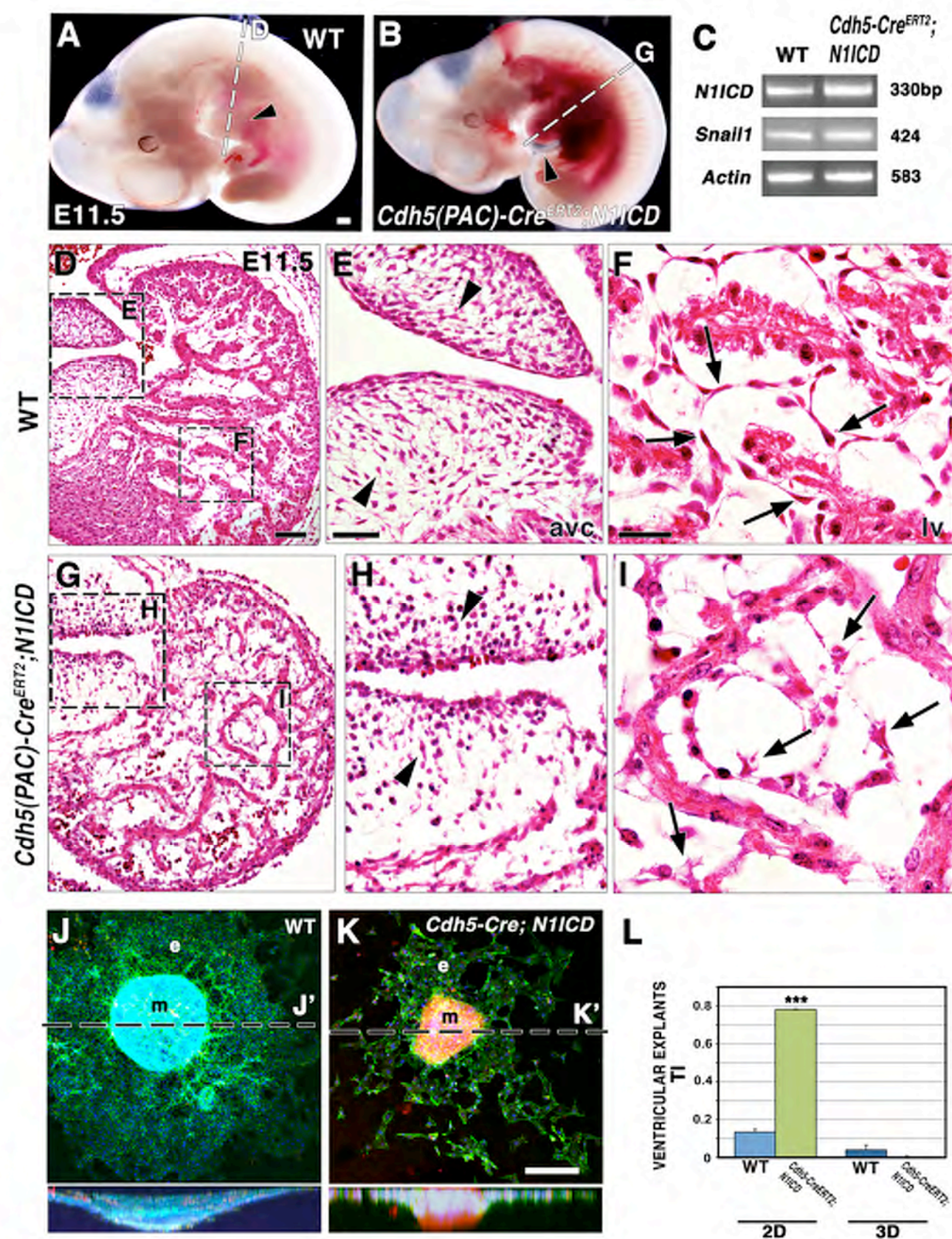


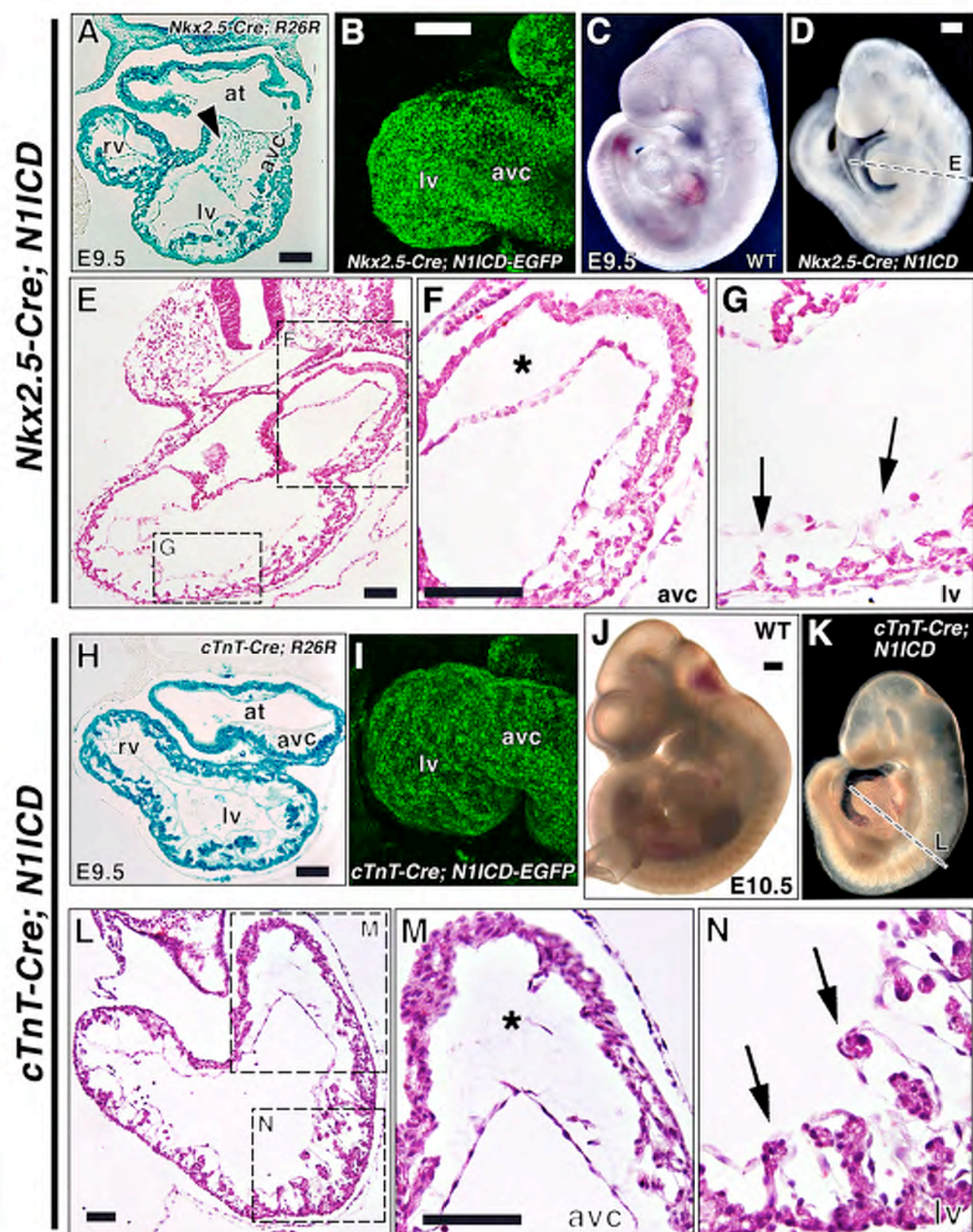
Luna-Zurita\_Suppl. Figure 5

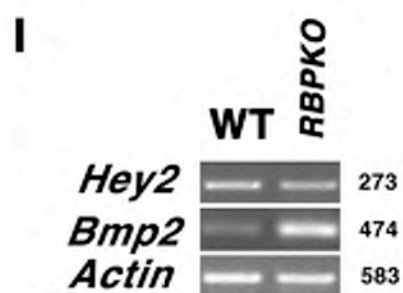
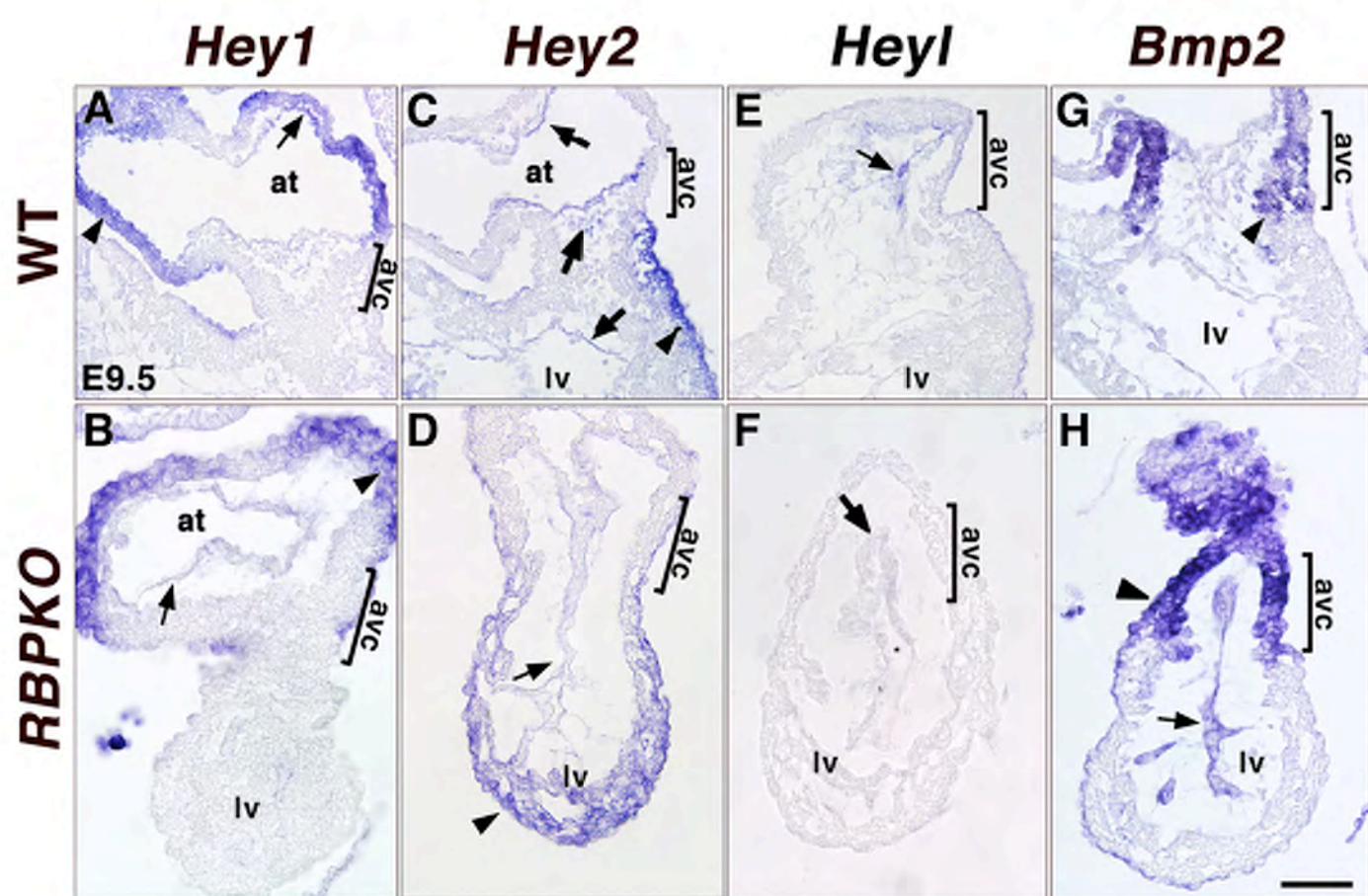


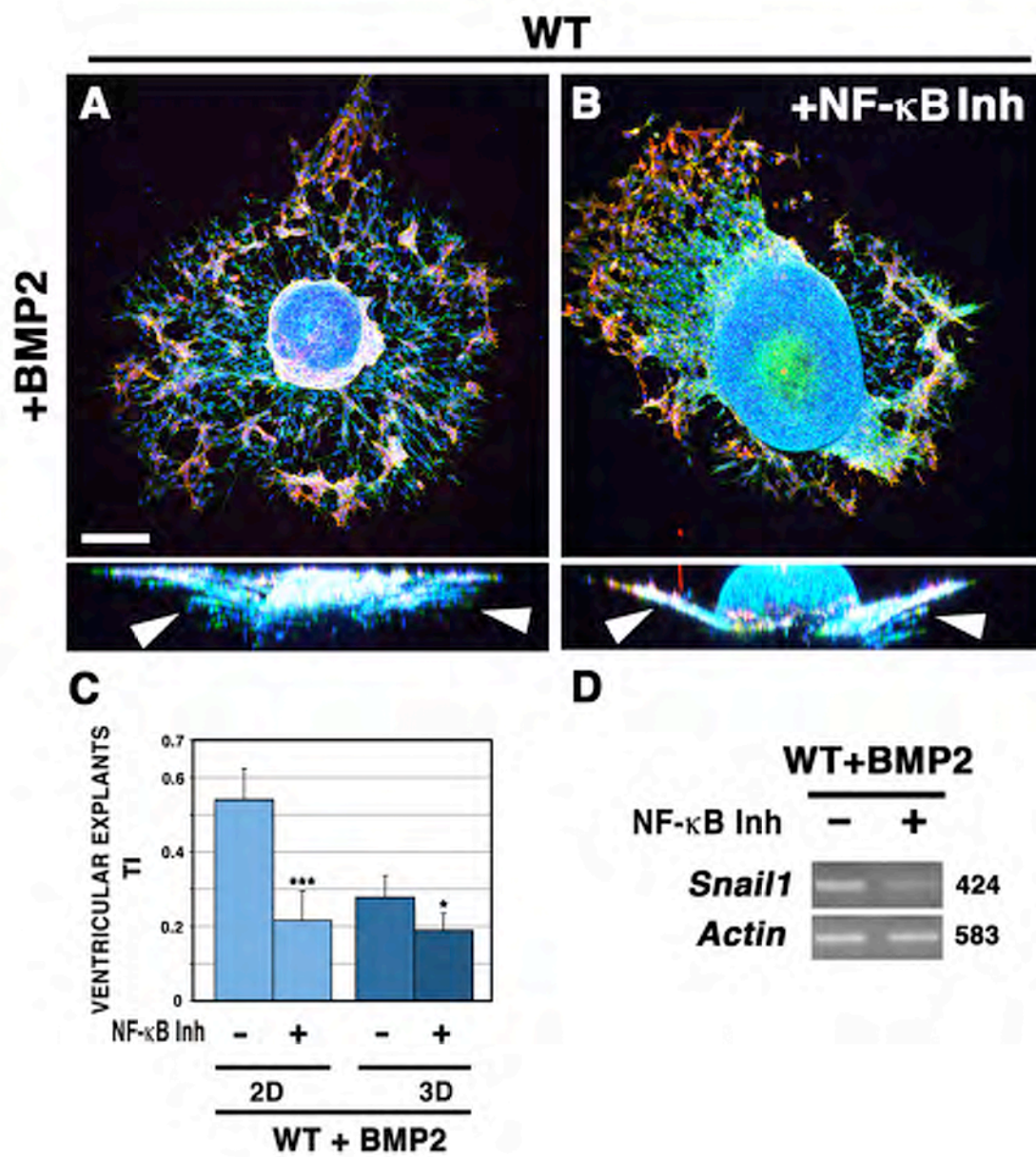


Luna-Zurita\_Suppl. Figure 7

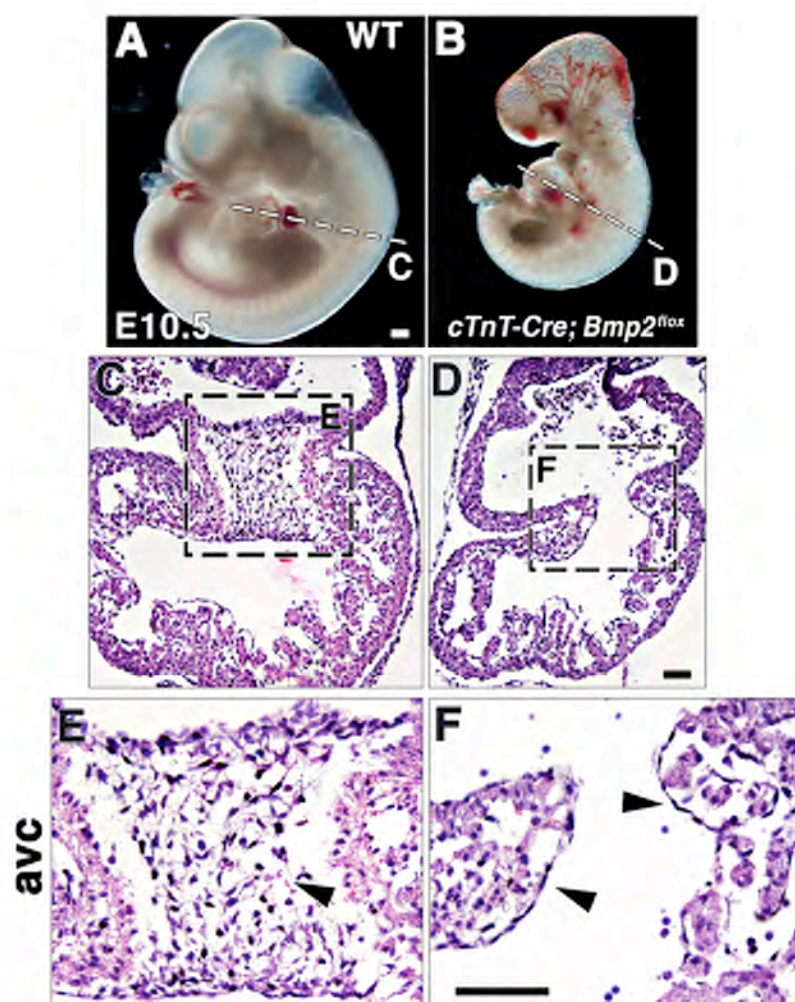


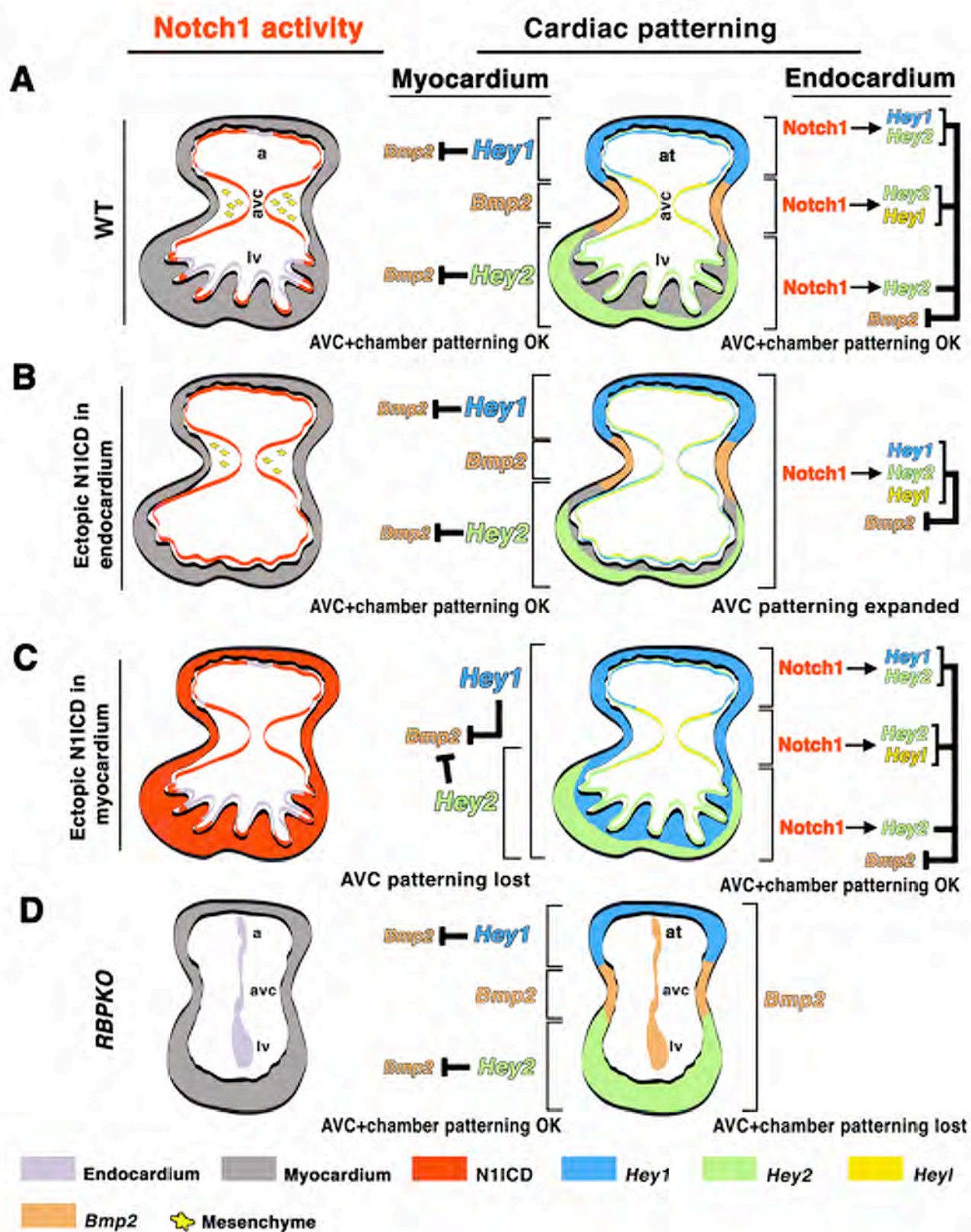






Luna-Zurita\_Suppl. Figure 11





Luna-Zurita et al. **Supplemental Table 1:** Differentially expressed genes in the heart of *Tie2-CRE; NIICD* embryos that are involved in cell migration, invasion and Notch signaling.

<b>Gene symbol</b>	<b>Gene</b>	<b>Affymetrix probe-set ID</b>	<b>Ref. Seq ID</b>	<b>WT Avg_log2 exp</b>	<b>NIICD Avg_log2 exp</b>	<b>Log 2 ratio</b>	<b>Adjusted p value (FDR)</b>	<b>Cellular Function</b>	<b>Reference</b>
<i>Snail2</i>	Snail2	1447643_x_at	NM_011415	7.08	8.11	1.03	0.023	EMT	(1).
<i>Twist2</i>	Twist homolog 2	1448925_at	NM_007855	5.21	5.95	0.74	0.031	EMT	(2)
<i>Bmp6</i>	Bone Morphogenetic Protein 6	1450759_at	NM_007556	5.82	6.49	0.67	0.029	EMT	(3)
<i>Bmpr1a/Alk3</i>	Bone Morphogenetic Protein Receptor 1A	1425491_at	NM_009758	7.17	7.89	0.72	0.051	EMT	(4)
<i>Bmpr1b/Alk6</i>	Bone Morphogenetic Protein Receptor 1B	1437312_at	NM_007560	4.62	5.14	0.52	0.039	EMT	(5)
<i>Cxcl7</i>	chemokine (C-X-C motif) ligand 7	1418480_at	NM_023785	3.79	6.04	2.25	0.015	Cell Migration	(6)
<i>Cxcr4</i>	chemokine (C-X-C motif) receptor 4	1448710_at	NM_009911	4.65	6.4	1.75	0.001	Cell Migration, Metastasis	(7)
<i>CD47</i>	CD47 antigen	1419554_at	NM_010581	7.66	8.64	0.98	0.031	Transendothelial Migration of T cells	(8)
<i>Cyr61</i>	cysteine rich protein 61	1416039_x_at	NM_010516	7.63	8.71	1.08	0.010	Endothelial Migration	(9)

<b><i>Foxo3a</i></b>	forkhead box O3a	1434832_at	NM_019740	5.93	7.13	1.2	0.017	Endothelial Migration	(10)
<b><i>Tiam1</i></b>	T-cell lymphoma invasion and metastasis 1	1418057_at	NM_009384	7.39	8.24	0.85	0.037	Proinvasive Factor	(11)
<b><i>Anxa2</i></b>	annexin A2	1419091_a_at	NM_007585	10	11.11	1.11	0.006	Migration, Adhesion	(12)
<b><i>Anxa4</i></b>	annexin A4	1421223_a_at	NM_013471	4.68	6.79	2.11	0.002	Cell migration	(13)
<b><i>Thbs1</i></b>	thrombospondin 1	1460302_at	NM_011580	5.62	7.05	1.43	0.002	Cell migration	(14)
<b><i>Smoc2</i></b>	SPARC related modular calcium binding 2	1415935_at	NM_022315	5.07	6.12	1.05	0.028	Endothelial migration	(15)
<b><i>Malat1</i></b>	metastasis associated lung adenocarcinoma transcript 1	1429060_at	NR_002847	6.88	8.28	1.4	0.028	Metastasis	(16)
<b><i>P4ha1</i></b>	procollagen-proline, 2-oxoglutarate 4-dioxygenase (proline 4-hydroxylase), alpha 1 polypeptide	1426519_at	NM_011030	5.51	7.28	1.77	0.008	Collagen synthesis	(17)
<b><i>Plod2</i></b>	procollagen lysine, 2-oxoglutarate 5-dioxygenase 2	1416686_at	NM_011961	7.40	9.19	1.79	0.012	Collagen synthesis	(18)
<b><i>Dkk3</i></b>	dickkopf homolog 3	1448669_at	NM_015814	7.44	8.56	1.12	0.006	Invasion modulation	(19)
<b><i>Nppa</i></b>	natriuretic peptide precursor type A	1456062_at	NM_008725	11.71	12.59	0.88	0.006	Chamber development	(20)
<b><i>Vwf</i></b>	Von Willebrand factor homolog	1435386_at	NM_011708	6.60	7.84	1.24	0.008	Endothelial differentiation and	(21)

								function	
<b><i>Irx6</i></b>	Iroquois related homeobox 6	1427383_at	NM_022428	5.07	6.27	1.20	0.006	transcriptional regulation	(22)
<b><i>Hey1</i></b>	hairy/enhancer-of-split related with YRPW motif 1	1415999_at	NM_010423	7.93	8.75	0.82	0.037	Notch target, Cardiac EMT	(23, 24)
<b><i>Hey2</i></b>	hairy/enhancer-of-split related with YRPW motif 2	1418106_at	NM_013904	7.24	8.13	0.89	0.084	Notch target, AV valve development	(25, 26)
<b><i>Heyl</i></b>	hairy/enhancer-of-split related with YRPW motif-like	1419302_at	NM_013905	4.00	5.13	1.13	0.011	Notch target, Cardiac EMT	(24)
<b><i>Hand2</i></b>	heart and neural crest derivatives expressed transcript 2	1436041_at	XM_001475550	10.23	9.40	-0.83	0.011	Chamber development	(27, 28)
<b><i>Notch4</i></b>	Notch gene homolog 4	1449146_at	NM_010929	5.30	6.80	1.50	0.063	Endothelial Notch receptor	(29)
<b><i>c-Myc</i></b>	myelocytomatosis oncogene	1424942_a_at	NM_010849	5.91	6.69	0.78	0.036	Oncogene, Notch target	(30)
<b><i>Nrarp</i></b>	Notch-regulated ankyrin repeat protein	1417985_at	NM_025980	6.46	7.82	1.36	0.055	Notch target	(31)

## References

1. Niessen, K., Fu, Y., Chang, L., Hoodless, P.A., McFadden, D., and Karsan, A. 2008. Slug is a direct Notch target required for initiation of cardiac cushion cellularization. *J Cell Biol* 182:315-325.

2. Ansieau, S., Bastid, J., Doreau, A., Morel, A.P., Bouchet, B.P., Thomas, C., Fauvet, F., Puisieux, I., Doglioni, C., Piccinin, S., et al. 2008. Induction of EMT by twist proteins as a collateral effect of tumor-promoting inactivation of premature senescence. *Cancer Cell* 14:79-89.
3. Kim, R.Y., Robertson, E.J., and Solloway, M.J. 2001. Bmp6 and Bmp7 are required for cushion formation and septation in the developing mouse heart. *Dev Biol* 235:449-466.
4. Song, L., Fassler, R., Mishina, Y., Jiao, K., and Baldwin, H.S. 2007. Essential functions of Alk3 during AV cushion morphogenesis in mouse embryonic hearts. *Dev Biol* 301:276-286.
5. Okagawa, H., Markwald, R.R., and Sugi, Y. 2007. Functional BMP receptor in endocardial cells is required in atrioventricular cushion mesenchymal cell formation in chick. *Dev Biol* 306:179-192.
6. Kalwitz, G., Endres, M., Neumann, K., Skriner, K., Ringe, J., Sezer, O., Sittinger, M., Haupl, T., and Kaps, C. 2009. Gene expression profile of adult human bone marrow-derived mesenchymal stem cells stimulated by the chemokine CXCL7. *Int J Biochem Cell Biol* 41:649-658.
7. Vasyutina, E., Stebler, J., Brand-Saberi, B., Schulz, S., Raz, E., and Birchmeier, C. 2005. CXCR4 and Gab1 cooperate to control the development of migrating muscle progenitor cells. *Genes Dev* 19:2187-2198.
8. Stefanidakis, M., Newton, G., Lee, W.Y., Parkos, C.A., and Luscinskas, F.W. 2008. Endothelial CD47 interaction with SIRPgamma is required for human T-cell transendothelial migration under shear flow conditions in vitro. *Blood* 112:1280-1289.
9. Athanasopoulos, A.N., Schneider, D., Keiper, T., Alt, V., Pendurthi, U.R., Liegibel, U.M., Sommer, U., Nawroth, P.P., Kasperk, C., and Chavakis, T. 2007. Vascular endothelial growth factor (VEGF)-induced up-regulation of CCN1 in osteoblasts mediates proangiogenic activities in endothelial cells and promotes fracture healing. *J Biol Chem* 282:26746-26753.
10. Potente, M., Urbich, C., Sasaki, K., Hofmann, W.K., Heeschen, C., Aicher, A., Kollipara, R., DePinho, R.A., Zeiher, A.M., and Dimmeler, S. 2005. Involvement of Foxo transcription factors in angiogenesis and postnatal neovascularization. *J Clin Invest* 115:2382-2392.
11. Costantini, D.L., Arruda, E.P., Agarwal, P., Kim, K.H., Zhu, Y., Zhu, W., Lebel, M., Cheng, C.W., Park, C.Y., Pierce, S.A., et al. 2005. The homeodomain transcription factor Irx5 establishes the mouse cardiac ventricular repolarization gradient. *Cell* 123:347-358.
12. de Graauw, M., Tijdens, I., Smeets, M.B., Hensbergen, P.J., Deelder, A.M., and van de Water, B. 2008. Annexin A2 phosphorylation mediates cell scattering and branching morphogenesis via cofilin Activation. *Mol Cell Biol* 28:1029-1040.
13. Zimmermann, U., Balabanov, S., Giebel, J., Teller, S., Junker, H., Schmoll, D., Protzel, C., Scharf, C., Kleist, B., and Walther, R. 2004. Increased expression and altered location of annexin IV in renal clear cell carcinoma: a possible role in tumour dissemination. *Cancer Lett* 209:111-118.
14. Motegi, K., Harada, K., Ohe, G., Jones, S.J., Ellis, I.R., Crouch, D.H., Schor, S.L., and Schor, A.M. 2008. Differential involvement of TGF-beta1 in mediating the motogenic effects of TSP-1 on endothelial cells, fibroblasts and oral tumour cells. *Exp Cell Res* 314:2323-2333.
15. Rocnik, E.F., Liu, P., Sato, K., Walsh, K., and Vaziri, C. 2006. The novel SPARC family member SMOC-2 potentiates angiogenic growth factor activity. *J Biol Chem* 281:22855-22864.
16. Ji, P., Diederichs, S., Wang, W., Boing, S., Metzger, R., Schneider, P.M., Tidow, N., Brandt, B., Buerger, H., Bulk, E., et al. 2003. MALAT-1, a novel noncoding RNA, and thymosin beta4 predict metastasis and survival in early-stage non-small cell lung cancer. *Oncogene* 22:8031-8041.

17. Holster, T., Pakkanen, O., Soininen, R., Sormunen, R., Nokelainen, M., Kivirikko, K.I., and Myllyharju, J. 2007. Loss of assembly of the main basement membrane collagen, type IV, but not fibril-forming collagens and embryonic death in collagen prolyl 4-hydroxylase I null mice. *J Biol Chem* 282:2512-2519.
18. van der Slot, A.J., Zuurmond, A.M., Bardoel, A.F., Wijmenga, C., Pruijs, H.E., Silence, D.O., Brinckmann, J., Abraham, D.J., Black, C.M., Verzijl, N., et al. 2003. Identification of PLOD2 as telopeptide lysyl hydroxylase, an important enzyme in fibrosis. *J Biol Chem* 278:40967-40972.
19. Saeb-Parsy, K., Veerakumarasivam, A., Wallard, M.J., Thorne, N., Kawano, Y., Murphy, G., Neal, D.E., Mills, I.G., and Kelly, J.D. 2008. MT1-MMP regulates urothelial cell invasion via transcriptional regulation of Dickkopf-3. *Br J Cancer* 99:663-669.
20. Houweling, A.C., Somi, S., Van Den Hoff, M.J., Moorman, A.F., and Christoffels, V.M. 2002. Developmental pattern of ANF gene expression reveals a strict localization of cardiac chamber formation in chicken. *Anat Rec* 266:93-102.
21. Sadler, J.E. 1998. Biochemistry and genetics of von Willebrand factor. *Annu Rev Biochem* 67:395-424.
22. Mummehoff, J., Houweling, A.C., Peters, T., Christoffels, V.M., and Ruther, U. 2001. Expression of Irx6 during mouse morphogenesis. *Mech Dev* 103:193-195.
23. Nakagawa, O., McFadden, D.G., Nakagawa, M., Yanagisawa, H., Hu, T., Srivastava, D., and Olson, E.N. 2000. Members of the HRT family of basic helix-loop-helix proteins act as transcriptional repressors downstream of Notch signaling. *Proc Natl Acad Sci U S A* 97:13655-13660.
24. Fischer, A., Steidl, C., Wagner, T.U., Lang, E., Jakob, P.M., Friedl, P., Knobloch, K.P., and Gessler, M. 2007. Combined loss of Hey1 and HeyL causes congenital heart defects because of impaired epithelial to mesenchymal transition. *Circ Res* 100:856-863.
25. Kokubo, H., Miyagawa-Tomita, S., Tomimatsu, H., Nakashima, Y., Nakazawa, M., Saga, Y., and Johnson, R.L. 2004. Targeted disruption of hesr2 results in atrioventricular valve anomalies that lead to heart dysfunction. *Circ Res* 95:540-547.
26. Kokubo, H., Miyagawa-Tomita, S., Nakazawa, M., Saga, Y., and Johnson, R.L. 2005. Mouse hesr1 and hesr2 genes are redundantly required to mediate Notch signaling in the developing cardiovascular system. *Dev Biol* 278:301-309.
27. Srivastava, D., Thomas, T., Lin, Q., Kirby, M.L., Brown, D., and Olson, E.N. 1997. Regulation of cardiac mesodermal and neural crest development by the bHLH transcription factor, dHAND. *Nat Genet* 16:154-160.
28. McFadden, D.G., Barbosa, A.C., Richardson, J.A., Schneider, M.D., Srivastava, D., and Olson, E.N. 2005. The Hand1 and Hand2 transcription factors regulate expansion of the embryonic cardiac ventricles in a gene dosage-dependent manner. *Development* 132:189-201.
29. Krebs, L.T., Xue, Y., Norton, C.R., Shutter, J.R., Maguire, M., Sundberg, J.P., Gallahan, D., Closson, V., Kitajewski, J., Callahan, R., et al. 2000. Notch signaling is essential for vascular morphogenesis in mice. *Genes Dev* 14:1343-1352.
30. Weng, A.P., Millholland, J.M., Yashiro-Ohtani, Y., Arcangeli, M.L., Lau, A., Wai, C., Del Bianco, C., Rodriguez, C.G., Sai, H., Tobias, J., et al. 2006. c-Myc is an important direct target of Notch1 in T-cell acute lymphoblastic leukemia/lymphoma. *Genes Dev* 20:2096-2109.
31. Krebs, L.T., Deftos, M.L., Bevan, M.J., and Gridley, T. 2001. The Nrarp gene encodes an ankyrin-repeat protein that is transcriptionally regulated by the notch signaling pathway. *Dev Biol* 238:110-119.

**Supplemental Table 2: Genotyping primers**

Gene	Primers set (5' to 3')	Annealing temp. (°C)	Product length	Ref.
<i>R26N1ICD</i>	AAAGTCGCTCTGAGTTGTTAT GAAAGACCGCGAAGAGTTTG	55	317	(1)
<i>RBPJk</i>	CAGTGGGGAGCATTTCACCAT GAGGAAATTGCATCGCATTGTTCGAG	55	415	(2)-
<i>Bmp2<sup>fllox</sup></i>	GTGTGGTCCACCGCATCAC GGCAGACATTGTATCTCTAGG	55	545	(3)
<i>Tie2-Cre</i>	GGGAAGTCGCAAAGTTGTGAGTT CTAGAGCCTGTTTTGCACGTTTC	60	500	(4)
<i>Nkx2.5-Cre</i>	GCGCACTCACTTTAATGGGAAGAG GCCCTGTCCCTCAGATTTTCACACC	60	583	(5)
<i>cTnT-Cre</i>	TACTCAAGAACTACGGGCTGC GCACTCCAGCTTGTTCCCGA	60	350	(6)
<i>Cdh5(PAC)-Cre<sup>ERT2</sup></i>	ACACCAGAGACGGAAATCCATC GCAGAACCTGAAGATGTTCCGC	62	500	This report

**References**

1. Murtaugh, L.C., Stanger, B.Z., Kwan, K.M., and Melton, D.A. 2003. Notch signaling controls multiple steps of pancreatic differentiation. *Proc Natl Acad Sci U S A* 100:14920-14925.
2. Oka, C., Nakano, T., Wakeham, A., de la Pompa, J.L., Mori, C., Sakai, T., Okazaki, S., Kawaichi, M., Shiota, K., Mak, T.W., et al. 1995. Disruption of the mouse RBP-J kappa gene results in early embryonic death. *Development* 121:3291-3301.
3. Tsuji, K., Bandyopadhyay, A., Harfe, B.D., Cox, K., Kakar, S., Gerstenfeld, L., Einhorn, T., Tabin, C.J., and Rosen, V. 2006. BMP2 activity, although dispensable for bone formation, is required for the initiation of fracture healing. *Nat Genet* 38:1424-1429.
4. Kisanuki, Y.Y., Hammer, R.E., Miyazaki, J., Williams, S.C., Richardson, J.A., and Yanagisawa, M. 2001. Tie2-Cre transgenic mice: a new model for endothelial cell-lineage analysis in vivo. *Dev Biol* 230:230-242.
5. Stanley, E.G., Biben, C., Elefanty, A., Barnett, L., Koentgen, F., Robb, L., and Harvey, R.P. 2002. Efficient Cre-mediated deletion in cardiac progenitor cells conferred by a 3'UTR-ires-Cre allele of the homeobox gene *Nkx2-5*. *Int J Dev Biol* 46:431-439.
6. Jiao, K., Kulesa, H., Tompkins, K., Zhou, Y., Batts, L., Baldwin, H.S., and Hogan, B.L. 2003. An essential role of *Bmp4* in the atrioventricular septation of the mouse heart. *Genes Dev* 17:2362-2367.

Luna-Zurita et al.

**Supplemental Table 3: RT-PCR primers**

Gene	Primers set (5' to 3')	Annealing temp. (°C)	Product length	Ref.
<i>Anf</i>	GGCAGAGACAGCAAACATCA TGCTTTTCAAGAGGGCAGAT	55	381	This report
<i>Bmp2</i>	GTGTGGTCCACCGCATCAC GGCAGACATTGTATCTCTAGG	65	474	(1)
<i>Bmp6</i>	CGCGTCTACAAGGACTGTGTGGT CGTACTCGGGATTCATAAGGTGGA	60	649	This report
<i>CD31</i>	TGCGATGGTGTATAACGTCACCTCCA GCTTGGCAGCGAAACACTAACACGTG	56	384	(2)
<i>Chisel</i>	CCAATCCAGAGAGCAGGGCTAAG GACTACTGTTACCTTTGGGGACA	56	294	This report
<i>c-Myc</i>	GTCTTCCCCTACCCGCTC CTGTCCAACCTTGCCCTC	62	404	(3)
<i>Connexin 43</i>	CTGCCTTTCGCTGTAACACT CGCTCAAGCTGAACCCATA	57	399	(4)
<i>Cxcr4</i>	ACATCTGTGACCGCCTTTACCC GCTGGAGTGAAAACCTGGAGGATT	60	506	This report
<i>Delta-like 4</i>	AAGGTGCCACTTCGGTTACAC AGATGCCCACAGGAGCTACAG	60	531	(5)
<i>Has2</i>	ATGGATCCGCAAAAATGGGGTGGAA GCGAATTCTAGTTGCATAGCCCAGA	51	450	(6)
<i>Hey1</i>	AGG GTG GGA TCA GTG TGC TGC TTC TCA AAG GCA CTG	56	355	(5)
<i>Hey2</i>	GAG GCA GTG ATG ACA TCC CCC TGA TGG CAT CCG AAG AGC	58	273	(5)
<i>Heyl</i>	GGTCCCCACTGCCTTTGAGA AGGATGGCGAGCTGACTGTTC	65	381	(7)
<i>Irx5</i>	CCACTCGCCACCGCCACCT GCCATAGTTCGTGTAGCCCGGATA	63	304	(8)
<i>Mlc2a</i>	AAGGGAAGGGTCCCATCAACTTCA AACAGTTGCTCTACCTCAGCAGGA	55	202	(9)
<i>Mlc2v</i>	ACTTCACCGTGTTCCCTCACGATGT	55	254	(9)

	TCCGTGGGTAATGATGTGGACCAA			
<i>NIICD</i>	GCTGACCTGCGCATGTCTGCCATG CATGTTGTCCTGGATGTTGGCATCTG	60	330	This report
<i>Nrarp</i>	AGATGGTGGAGCCCGTAATGGTT TCTCATACCAAGGCCAAGTACGC	64	517	This report
<i>Periostin</i>	GGCTGAAGATGGTTCCTCTC TTGACATTGAGGAATAACCA	56	574	(10)
<i>Snail1</i>	GGAAGCCCAACTATAGCGAGC CAGTTGAAGATCTTCCGCGAC	57	424	(11)
<i>Snail2</i>	GCGAACTGGACACACACAGTTAT CCCCAGTGTGAGTTCTAATGTGTCC	55	572	(12)
<i>Sox9</i>	GCAAGCTGGCAAAGTTGATCT GCTGCTCAGTTCACCGATG	65	106	(13)
<i>Tgfb2</i>	AATGTGCAGGATAATTGCTGC TTCGGGATTTATGGTGTGTA	55	130	This report
<i>Twist1</i>	CGGGTCATGGCTAACGTG CAGCTTGCCATCTTGGAGTC	60	196	(14)
<i>Twist2</i>	ACAAGCTCAGCAAGATCCAGACGC GTGAGGAGATGAGGGCACAGAAG	61	433	This report
<i>Vimentin</i>	CCCCCTCCTCACTTCTTTC AAGAGTGGCAGAGGACTGGA	57	136	(15)
<i>b-Actin</i>	GGACCTGGCTGGCCGGGACC GCGGTGCACGATGGAGGGGC	62	583	(16)

#### References:

1. Rivera-Feliciano, J., and Tabin, C.J. 2006. Bmp2 instructs cardiac progenitors to form the heart-valve-inducing field. *Dev Biol* 295:580-588.
2. Ohneda, O., Fennie, C., Zheng, Z., Donahue, C., La, H., Villacorta, R., Cairns, B., and Lasky, L.A. 1998. Hematopoietic stem cell maintenance and differentiation are supported by embryonic aorta-gonad-mesonephros region-derived endothelium. *Blood* 92:908-919.
3. Laybutt, D.R., Weir, G.C., Kaneto, H., Lebet, J., Palmiter, R.D., Sharma, A., and Bonner-Weir, S. 2002. Overexpression of c-Myc in beta-cells of transgenic mice causes proliferation and apoptosis, downregulation of insulin gene expression, and diabetes. *Diabetes* 51:1793-1804.
4. Husøy, T., Cruciani, V., Knutsen, H.K., Mikalsen, S.O., Olstorn, H.B., and Alexander, J. 2003. Cells heterozygous for the ApcMin mutation have decreased gap junctional intercellular communication and connexin43 level, and reduced microtubule polymerization. *Carcinogenesis* 24:643-650.
5. Timmerman, L.A., Grego-Bessa, J., Raya, A., Bertran, E., Perez-Pomares, J.M., Diez, J., Aranda, S., Palomo, S., McCormick, F., Izpisua-Belmonte, J.C., et al. 2004. Notch promotes epithelial-mesenchymal transition during cardiac development and oncogenic transformation. *Genes Dev* 18:99-115.
6. Spicer, A.P., Augustine, M.L., and McDonald, J.A. 1996. Molecular cloning and characterization of a putative mouse hyaluronan synthase. *J Biol Chem* 271:23400-23406.

7. Wang, W., Campos, A.H., Prince, C.Z., Mou, Y., and Pollman, M.J. 2002. Coordinate Notch3-hairy-related transcription factor pathway regulation in response to arterial injury. Mediator role of platelet-derived growth factor and ERK. *J Biol Chem* 277:23165-23171.
8. Grego-Bessa, J., Luna-Zurita, L., del Monte, G., Bolos, V., Melgar, P., Arandilla, A., Garratt, A.N., Zang, H., Mukoyama, Y.S., Chen, H., et al. 2007. Notch signaling is essential for ventricular chamber development. *Dev Cell* 12:415-429.
9. Kattman, S.J., Huber, T.L., and Keller, G.M. 2006. Multipotent flk-1+ cardiovascular progenitor cells give rise to the cardiomyocyte, endothelial, and vascular smooth muscle lineages. *Dev Cell* 11:723-732.
10. Kruzynska-Frejtag, A., Machnicki, M., Rogers, R., Markwald, R.R., and Conway, S.J. 2001. Periostin (an osteoblast-specific factor) is expressed within the embryonic mouse heart during valve formation. *Mech Dev* 103:183-188.
11. Veltmaat, J.M., Orelia, C.C., Ward-Van Oostwaard, D., Van Rooijen, M.A., Mummery, C.L., and Defize, L.H. 2000. Snail is an immediate early target gene of parathyroid hormone related peptide signaling in parietal endoderm formation. *Int J Dev Biol* 44:297-307.
12. Inoue, A., Seidel, M.G., Wu, W., Kamizono, S., Ferrando, A.A., Bronson, R.T., Iwasaki, H., Akashi, K., Morimoto, A., Hitzler, J.K., et al. 2002. Slug, a highly conserved zinc finger transcriptional repressor, protects hematopoietic progenitor cells from radiation-induced apoptosis in vivo. *Cancer Cell* 2:279-288.
13. Notarnicola, C., Malki, S., Berta, P., Poulat, F., and Boizet-Bonhoure, B. 2006. Transient expression of SOX9 protein during follicular development in the adult mouse ovary. *Gene Expr Patterns* 6:695-702.
14. Thuault, S., Valcourt, U., Petersen, M., Manfioletti, G., Heldin, C.H., and Moustakas, A. 2006. Transforming growth factor-beta employs HMGA2 to elicit epithelial-mesenchymal transition. *J Cell Biol* 174:175-183.
15. Shaw, A., Papadopoulos, J., Johnson, C., and Bushman, W. 2006. Isolation and characterization of an immortalized mouse urogenital sinus mesenchyme cell line. *Prostate* 66:1347-1358.
16. Bi, W., Drake, C.J., and Schwarz, J.J. 1999. The transcription factor MEF2C-null mouse exhibits complex vascular malformations and reduced cardiac expression of angiotensin 1 and VEGF. *Dev Biol* 211:255-267.